Fluorine-Doped Solid-State Electrolytes in Lithium-ion Batteries: Potential for a Cleaner Future

Kunj Kapur

Supervisor: Dr. Karen E. Johnston

Department of Chemistry, Durham University

Fluorine-Doped Solid-State Electrolytes for Lithium-ion Batteries: Potential for a Cleaner Future

Kunj Kapur

Department of Chemistry, Durham University, Durham UK

Email: kunj.kapur@durham.ac.uk

Abstract

Current Lithium-ion (Li-ion) batteries utilise liquid electrolytes that conduct ions. However, these pose several significant issues, including safety, thermal runaway and toxicity. To circumvent these challenges, solid ion conductors, known as solid-state electrolytes (SSEs) are being developed, which promise greater safety and either equivalent or better performance. Lithium- and sodium-rich anti-perovskites (LiRAPs and NaRAPs) are exciting classes of materials with great potential to be solid electrolytes in the future.

In recent years, the halide substitution of LiRAPs has gained considerable attention owing to their enhanced ion mobility and ionic conductivity. The research presented here focuses on four series of lithium halide hydroxide anti-pervoskite electrolytes: $Li_2(OH)_{1-x}F_xCl$, $Li_2(OH)_{1-x}F_xBr$, $Li_2(OH)Cl_{1-x}Br_x$ and $Li_2(OH)_{1-x}F_xBr_{1-y}Cl_y$, with $0.0 \leq x \leq 1.0$, which have been prepared via traditional solid-state methods. The successful incorporation of fluoride ions onto the hydroxide sites, thereby creating vacant sites, is

supported by solid-state NMR studies. This essay begins by introducing SSEs before moving on to outline some of the main challenges faced in developing LiRAPs for use as SSEs. The synthetic methods employed are explored in detail before the data acquired and results obtained are discussed.

1 Introduction

With a growing population, greater geopolitical clout and increased extreme weather conditions, the climate change crisis needs to be combatted with credibility and urgency. The energy sector contributes to 76% of the world's greenhouse gas emissions and, at the current rate, all non-renewable resources will be exhausted by 2060 and the demand for energy will double by 2050. According to the International Energy Agency (IEA), sustainable energy goals will only be met if 10000 GWh of required energy is achieved by 2040. Extreme disasters like wildfires, tsunamis, etc. continue to impact the world and have significant social, environmental and economic impact, particularly in developing regions. Although renewable energy contributes to almost 50% of the growth in global energy supplies, the transition needed to be able to store this energy efficiently before its distribution requires improved technology, such as lithium- and/or sodium-ions batteries. Modern society needs to provide a dependable and sustainable energy supply for both current and future generations.

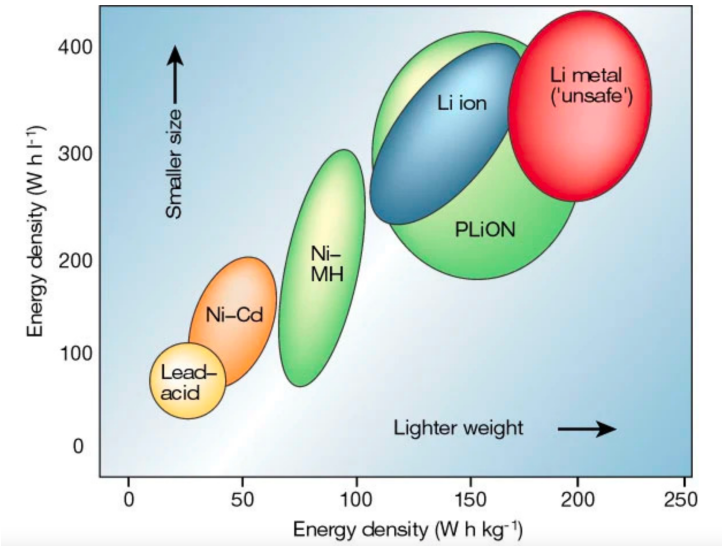

Figure 1: Ragone plot of lithium batteries shows the high energy density of Li-ion batteries in comparison to conventional batteries.[1]

Electrochemical batteries have the potential to reduce global emissions in both the transport and power sectors by 30% in the next ten years, thereby facilitating the energy transition from fossil fuels to emission-free energies by acting as an efficient method of energy storage. Sustainable energy will bridge the gap for people without electricity by 70% by providing electricity to 850 million people worldwide, thereby improving productivity and quality of life, with a significant and positive impact on the environment. Current research in intermittent energy such as solar and wind power, has been very progressive and promising towards a low-carbon future, but they are currently unable to meet energy demands at certain times of the year. It is pertinent that the drive to overcome the environmental impact of fossil fuels involves the development of alternative energy-storage technologies.

2 Batteries

2.1 Components of a Battery

A battery is composed of one or more electrochemical cells which store chemical energy and convert it to electrical energy when required. Each cell contains two electrodes, an anode (negative) and a cathode (positive), separated by an electrolyte which permits ion movement. Oxidation at the anode results in the production of ions (which flow through the electrolyte to the cathode to be used up during reduction) and electrons (which travel through the external circuit). Therefore, it is essential that anodes are good reducing agents (i.e., able to lose electrons easily) and cathodes are good oxidising agents (i.e., able to accept electrons easily). Metallic current collectors (typically composed of aluminium or copper) are used to transfer current between the electrode and external circuit. Electrolytes prevent batteries from short-circuiting by acting as a separator, i.e., a physical barrier between the cathode and anode.

2.2 Types of Batteries

There are two main types of batteries: primary and secondary. Primary batteries are non-rechargeable that are charged during manufacture and discharged during use; they are single use as the chemical reaction taking place is irreversible. Alkaline and coin cell batteries are two common types of primary batteries. In contrast, secondary batteries can be recharged multiple times and can be restored to their charged state after being fully discharged. Common secondary batteries include lead-acid batteries, nickel-cadmium batteries and Li-ion batteries. Batteries must meet certain strict requirements before they can be used commercially, including high capacity, volumetric energy, power densities and ionic conductivity. Furthermore, secondary batteries have many requirements that must be kept in

mind, including lifespan and cycle stability, self-discharge, depth of discharge and charging time.

Materials within secondary batteries must be chemically stable over a range of operating conditions, such as time, temperature, and voltage. General batteries must operate safely from 0 ℃ - 40 ℃ and stored safely from −20 ℃ to 85 ℃. Battery degradation is a collection of events, complex chemical and physical processes, that impair the battery's ability to store charge and deliver power. A battery's state-of-health depends on different factors, such as rapid charging.

Lithium batteries have a high specific capacity and redox potential, resulting in high capacities and power densities. Li metal showcases high theoretical capacity (3860 mAh g^{-1}) and the lowest electrochemical potential (−3.04 V vs. a standard hydrogen electrode). Therefore, lithium metal is a very promising candidate for solid-state batteries (SSBs). However, for lithium-based batteries, the loss of ions available for charge-carrying is often the primary reason deterioration in battery performance. For example, the solid electrolyte interface (SEI), a layer that grows on the surface of the anode during operation, can result in the irreversible chemical loss of lithium. In addition, metallic lithium can also grow as dendrites (long thin metallic strands), which can pierce separators, resulting in short circuiting of the battery. The loss of lithium ions, cathode/anode and electrolyte can result in a capacity fade (i.e., the battery is unable to store power).

2.2 Lithium-ion Batteries

Developed in the 1990s, Li-ion batteries are a solution to earlier batteries employing organic solvents as electrolytes. Compared to other rechargeable batteries such as nickel-

cadmium or nickel-metal-hydride, Li-ion batteries have high energy densities (110-265 Wh/kg) and deliver up to three times higher voltages than Ni-Cd or Ni-MH. With a low need for maintenance and scheduled cycling and no memory effect they have potential in many applications.[2] Furthermore, they do not contain toxic cadmium, which makes their disposal much easier.

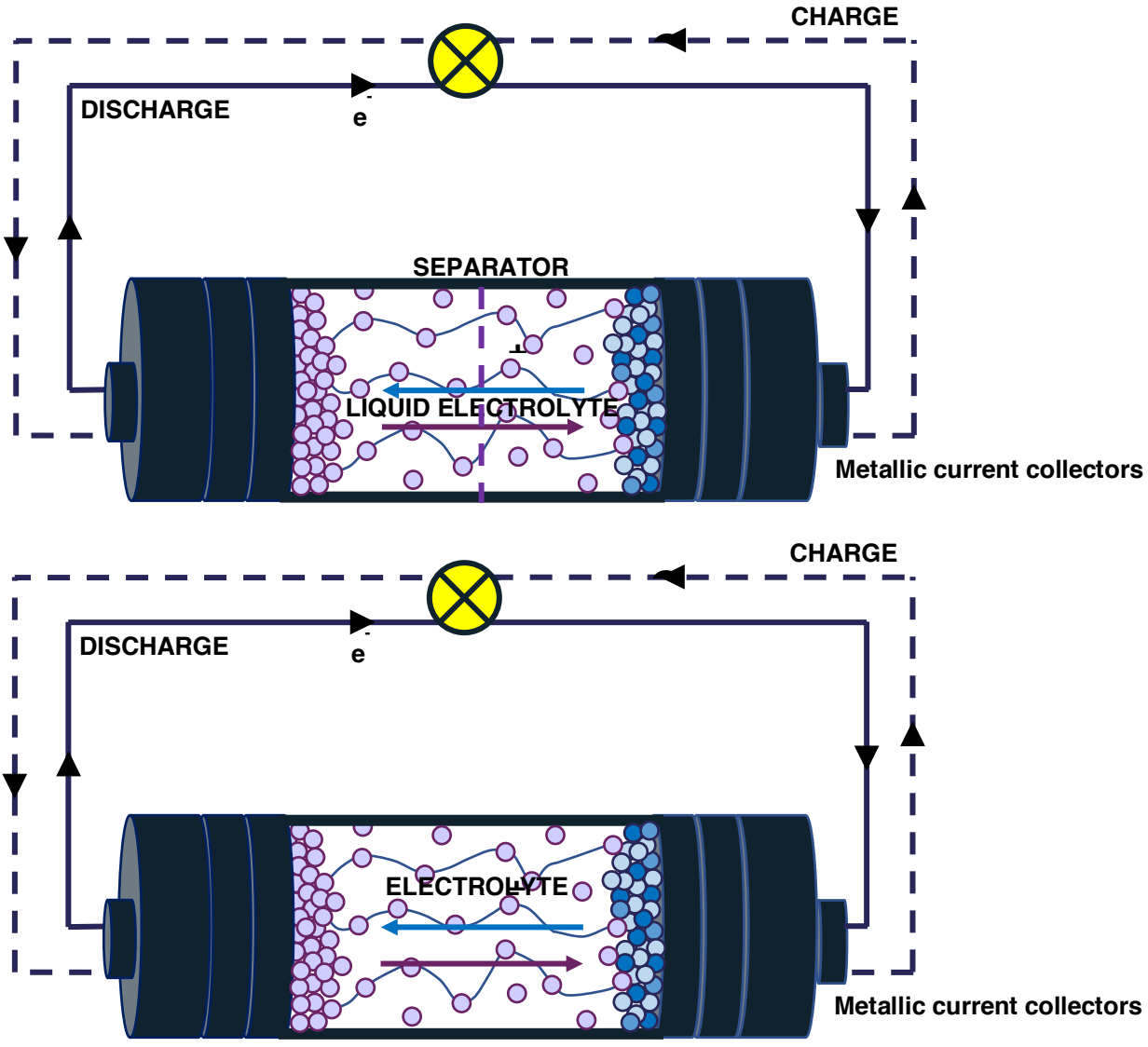

Figure 2: Schematic representation of a conventional battery and solid-state battery. The conventional battery is composed of liquid electrolytes with a separator, whilst the SSB is composed of two electrodes: Lithium anode and $LiCoO_2$ cathode, separated by a Li-ion conducting electrolyte of an anti-perovskite structure.

2.2.1 Cathode Materials

Commonly, intercalation materials are used in Li-ion batteries, as they can act as a solid host network to store guest Li ions, which can be added and removed reversibly. The host

network compounds could be metal chalcogenides, transition-metal oxides, and polyanion compounds. Intercalation materials have various crystal structures such as layered, spinel, olivine and tavorite.[3] The redox potential associated with intercalation should be as high as possible. Goodenough first introduced $LiCoO_2$ as a cathode material. However, initially, it didn't attract much attention owing to the high cost of cobalt. He then suggested the spinel $LiMnO_2$, which had limited applications due to the lack of safe and compatible anode materials. $LiCoO_2$ and $LiFePO_4$ are the current most widely used cathode materials in commercial Li-ion batteries due to their good cycle life (>500 cycles), high theoretical (274 mAh/g) and practical capacity (140 mAh/g). However, cobalt's toxicity and high material cost makes $LiCoO_2$ less attractive.

2.2.1 Anode Materials

Lithium metal anodes are unsuitable for lithium-ion batteries so specialised anode materials are used. The first commercial Li-ion battery paired graphite carbon anode with $LiCoO_2$. Graphite's layers are stacked either in the thermodynamically more stable ABAB sequence (hexagonal symmetry) or less stable ABCABC sequence (rhombohedral symmetry). The sp^2 hybridised graphene layers are linked by weak van der Waals forces and π–π interactions of the delocalised electron orbitals, which enables the efficient intercalation of Li ions into the layers. To accommodate a high lithium content, the single graphene layers slightly slide past each other, changing the ABABA stacking symmetry to an AIAIA stacking in the fully lithiated state (LiC_6).[4] This layered structure allows the intercalation of lithium ions into the anode upon charging. Due to its low delithiation potential, low cost, high abundance, high ionic and electric conductance, and low volume change upon intercalation, it is considered an attractive anode material. However, only one lithium ion can be inserted for every six carbon atoms, giving graphite a limited capacity. Theoretical calculations suggest the volume of the

graphite increases by ~10% after full lithiation, inevitably causing strain, stress and cracks in the electrode, thereby resulting in a reduction in performance.[5] Furthermore, a fast rate of charging can result in lithium plating onto the surface of the anode instead of intercalating with the graphite, causing an irreversible loss in capacity.

Due to the limited electrochemical window of liquid electrolytes, a lithium metal anode is not compatible, and can induce dendritic growth. Unstable electrolytes, mainly carbonate-based solvents, undergo reduction decomposition and contribute to the SEI, which can get out of control and break down, causing the lithium ions to become inactive, hence decreasing the coulombic efficiency of lithium.[6] [7]

2.3 Solid Electrolytes

Solid electrolytes greatly enhance the safety of the metal-ion batteries by complete removal of any liquid component, which pose possible leakage of flammable and potentially hazardous materials. Apart from reducing the safety concerns, SSEs also create robust batteries resistant to wear and tear. These provide a more stable voltage and decrease the self-discharge of the battery. In addition to the safety benefits, solid electrolytes have the potential to enable the use of lithium metal anodes, which will have enhanced energy densities and electrochemical windows. However, SSEs involve some challenges, particularly with their manufacturing costs and low power density.[8]

SSBs are like conventional batteries, in that they have an anode, cathode and electrolyte. The solid electrolyte here acts as an ionic insulator and separator. There are three main categories of SSEs: inorganic electrolytes, organic electrolytes, and composite electrolytes. Inorganic electrolytes exhibit high ionic conductivity with high thermal stability, due to inflexible crystal structure. However, the poor interfacial contact between the solid

electrolytes and lithium metal electrodes leads to exceptionally high internal resistance of the cells. Hence, they provide lower-than-expected performance. Organic polymers are very flexible due to their chemical and mechanical properties, so are employed with different battery designs. However, they have a low Li^+ conductivity with large ionic transfer resistance and undergo oxidation at high voltages. Many materials such as oxides, including perovskites, garnets, sulphides and phosphates are currently under investigation as possible solid electrolytes.[9] The development of hybrid electrolytes, i.e., those that are a combination of inorganic and organic electrolytes is therefore underway, however safety is an issue due to the flammability of organic polymers.

2.3.1 Anti-perovskites

First discovered in 1915, antiperovskites have been reported as excellent candidates for energy storage. These are a class of electronically inverted perovskites (they crystallise in a perovskite structure) with a general formula $X_3^+B^{2-}A^-$. The three-dimensional structure of anti-perovskites is comprised of corner-sharing BX_6 octahedra, with monovalent A^- anions and bivalent B^{2-} anions, which are 6-fold and 12-fold coordinated with the highly electropositive X metal's X^+ cations, respectively.

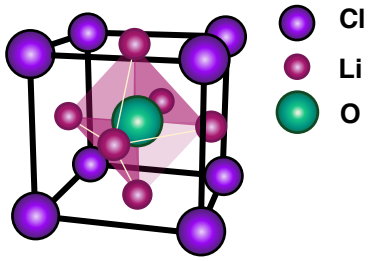

Figure 3: Anti-perovskite structure with overall geometry A_2BX_6.

As seen by their comprehensive properties, anti-perovskites (Figure 3) possess good reduction stability and low melting temperature, attracting attention towards the research of

their use in Na/Li ion batteries. Anti-perovskites can be further classified into four categories: lithium halide hydroxides, oxyhalide antiperovskites, cluster-based antiperovskites, and hydride-based antiperovskites. LiRAPs (Li-rich antiperovskites), NASICONS (sodium superionic conductors), and a new family of Li/Na rich antiperovskites have been reported as superionic conductors with high ionic conductivity, low electronic conductivity, good chemical and thermal stability, and a wide electrochemical window.[6]

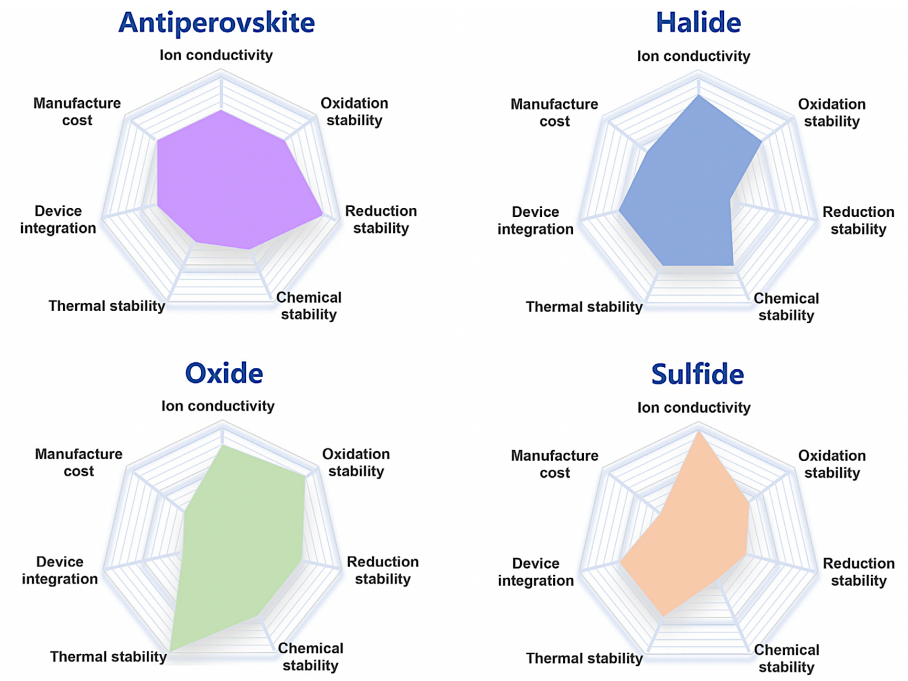

Figure 4: Radar plots show the performance properties of different types of SSEs: anti-perovskite, halide, oxide, and sulfides.[6]

2.3.1.1 Lithium-Rich Anti-perovskites (LiRAPs)

LiRAPs have the general formula Li_3OA, where A = Cl, Br, or I. The LiRAP Li_3OCl is reported to exhibit an ionic conductivity of 8.5×10^{-4} S cm^{-1} with an activation barrier of 0.26 eV, which can be improved by structural substitution. Along with high ionic conductivities, they have electrochemical windows greater than 5 V, good cyclability, low cost, non-flammable, environmentally friendly, and are recyclable. LiRAPs are stable in contact with

metallic lithium, so even higher voltage outputs can be achievement through the employment of Li-metal anodes. Halogen mixing of LiRAPs is reported to increase the Li ion conductivity to 1.94 × 10^{-3} S cm^{-1} and decrease the activation barrier to 0.18 eV in $LiOCl_{0.5}Br_{0.5}$ due to the increase in Li-O bond length, due to the larger Br being present.[10]

2.3.1.2 Fluorine-doping of LiRAPs

Doping refers to the substitution of fluoride (F^-) ions onto the hydroxide (OH^-) ion site. Yutau *et al*., reported that, upon the substitution of fluoride ions, the orthorhombic structure of the LiRAP is transformed into a cubic structure, increasing the electrochemical window to 9 V versus Li^+/Li. Fluorine doping increases the cubic tolerance factor, *t*:

$$t = \frac{X-Li}{\sqrt{2}(O-Li)}$$

where X-Li and O-Li are equilibrium lengths. Increasing *t* over 0.9 stabilises the cubic phase, hereby favouring the disordering of the OH^- orientation and reduces the number of hindering H^+ ions.[11]

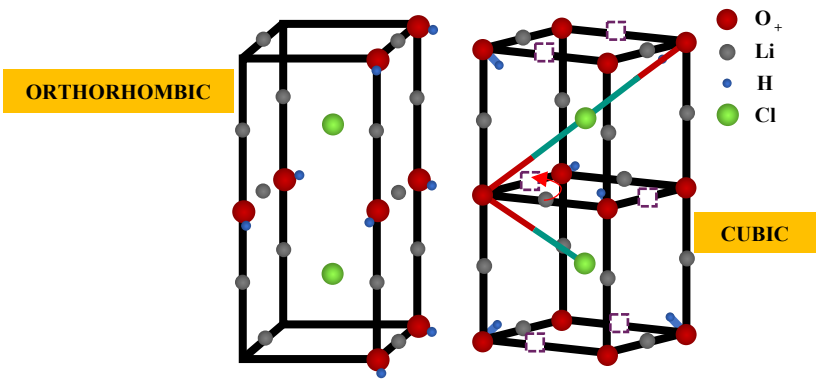

Figure 5: Li-ion hopping mechanism in the orthorhombic vs. cubic phase of LiRAP Li_2OHCl.

For Li_2OHCl, the Li^+ ions form 180° O–Li–O bonds in the cubic phase and H^+ ions get displaced from a cubic edge to form linear O-H-Cl bonds. A Li^+ ion 'hops' into a vacancy (purple box) through a triangular O^{2-} site (Figure 5). However, due to the coulombic repulsion and steric hindrance of the H^+ ions in the fixed O-H-Cl bond, the Li^+ jump is hindered. A

sudden phase change from orthorhombic to cubic at 35 °C results in the hydrogen bond randomly orientating to one of its eight nearest X^- neighbours due to rotations of the hydrogen bond, facilitating the decrease in activation energy for the Li hopping mechanism. Therefore, the substitution of F^- for an OH^- anion reduces the number of hindering H^+ ions and stabilises the more favourable cubic phase at room temperature. Furthermore, Br's larger size bends the O-H-Br bonds. Hence, the larger size Br^- anions significantly hinder the Li-ion movement by squeezing the Li-ion transport channel, hence increasing the activation energy.

2.3.1.3 Schottky and Frenkel Defects

Fluorinated lithium-rich anti-perovskites (F-LiRAP) are proposed to increase lithium-ion conductivity by creating Frenkel defects which facilitate the formation of lithium-rich and lithium-vacancy couples.[12] Heterogeneous doping results in lattice expansion and shrinkage of crystal structures due to varying atom radius and therefore bond lengths. Frenkel and Schottky defects are a probable source of these volume defects: they increase the ionic conductivity by increasing the mobility and concentration of charge and adjusting the local microstructure of the fluorine incorporated LiRAP.

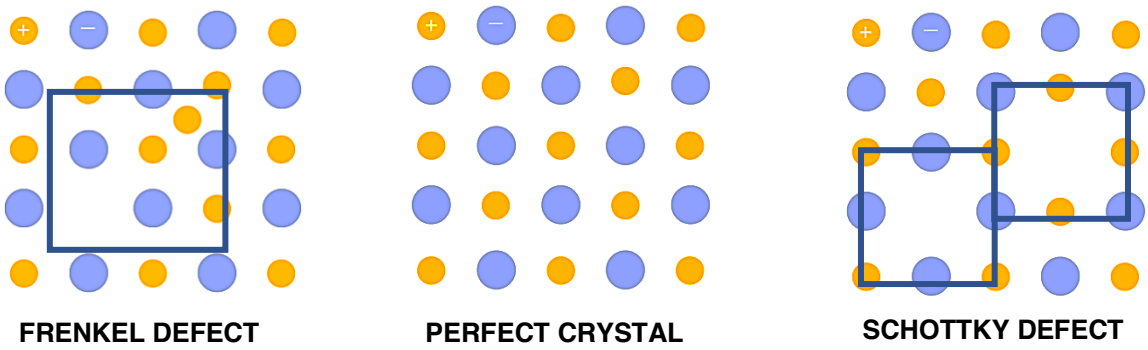

Figure 6: Structural description of different types of intrinsic defects: Frenkel and Schottky compared to the perfect crystal

Frenkel defects form when an atom or ion (usually cation) leaves its site in the lattice and becomes an interstitial by lodging in a nearby location, thus creating a vacancy at its original site. This is only possible if the cations are smaller in size than the anions. Schottky

defects occur when both the cation and anion leave their corresponding lattice sites and create a pair of vacancy defects. This usually happens when the difference in cation and anion size is small. These defects are thermal induced so the number of defects, thus the conductivity, increases with increasing temperature, as evidenced by the equations below.[13]

$$n_s = Ne^{\frac{-E_v}{kT}} \quad \text{(Schottky defects or vacancies)}$$

$$n_f = (NN')^{1/2} e^{\frac{-E_i}{2kT}} \quad \text{(Frenkel defects or vacancies)}$$

Where N is the total number of atoms and N' is the total number of interstitial sites

3 Synthesis

LiRAPs are highly hygroscopic and readily react with moisture in the air, leading to their decomposition. As a result, the preparation of LiRAPs must be conducted in an inert atmosphere. Two synthetic techniques were employed to produce four LiRAP series of samples from $0.0 \leq x \leq 1.0$, three of which are fluorine doped: (1) Heating reagents in a muffle furnace within an Ar-filled glovebox's inert atmosphere and (2) Heating reagents under vacuum using a Schlenk line setup.

The four compositions were prepared by stoichiometric calculations to find the mass of lithium salts: LiF, LiCl, LiBr and LiOH that should be incorporated. The fully balanced equations for the four samples are as stated below:

$$(1-x)\ Li(OH) + x\ LiF + LiCl \rightarrow Li_2(OH)_{1-x}F_xCl$$

$$(1-x)\ Li(OH) + x\ LiF + LiBr \rightarrow Li_2(OH)_{1-x}F_xBr$$

$$Li(OH) + (1-x)\ LiCl + x\ LiBr \rightarrow Li_2(OH)Cl_{1-x}Br_x$$

$$(1-x)\ Li(OH) + x\ LiF + (1-y)\ LiBr + y\ LiCl \rightarrow Li_2(OH)_{1-x}F_xBr_{1-y}Cl_y$$

3.1 Muffle Furnace in Argon-filled Glovebox

Stoichiometric quantities of LiCl (Alfa Aesar, ultra-dry, 99.9%), LiOH (Acros Organics, anhydrous, 98%), LiF (Acros Organics, anhydrous, 99.98%) and LiBr (Alfa Aesar, ultra-dry, 99.9%) were weighed out in an Ar-filled glovebox using an analytical balance and then ground together using a pestle and mortar. This powdered mixture was then placed in an alumina crucible and heated at 350 °C for 30 min in the muffle furnace, present in the Ar-glovebox. The furnace was allowed to cool down to room temperature once the reaction had completed. The recovered samples were then ground together, ready for loading into rotors for solid-state NMR analysis.

3.2 Schlenk Line

Stoichiometric quantities of LiCl (Alfa Aesar, ultra-dry, 99.9%), LiOH (Acros Organics, anhydrous, 98%), LiF (Acros Organics, anhydrous, 99.98%) and LiBr (Alfa Aesar, ultra-dry, 99.9%) were weighed out in an Ar-filled glovebox using an analytical balance and then ground together using a pestle and mortar. The powdered composition was then carefully loaded in an alumina crucible inside a sealed glass tube. This was then cycled out of the Ar-glovebox and connected to a conventional Schlenk line to be evacuated to 10^{-3} mbar for 1 hr. The glass reaction tube was inserted into a tube furnace and the reactants were heated to 350 °C for 30 mins before being allowed to cool back down to room temperature. Once cooled, the glass reaction tube was cycled back inside the Ar-filled glovebox and the sample was

recovered. The recovered sample was grounded again, as it had crystallised in many instances, ready for loading into rotors for solid-state NMR analysis.

4 Characterisation techniques

4.1 Solid-State NMR

Solid-state NMR spectra were acquired using the Bruker 400 Advance III HD spectrometer, with a wide-bore 11.7 T Oxford magnet, using 194.20 MHz for ^{7}Li (I = 3/2) as the Larmor frequency. Powdered samples were packed into 4.0 mm ZrO_2 rotors under an Ar atmosphere and placed into a Bruker 4.0 mm HX probe. A MAS rate of 10 kHz was employed. ^{7}Li chemical shifts were referenced to 1 M LiCl(aq). Different NMR probes were employed for different quadrupolar NMR nuclei, such as ^{7}Li, ^{35}Cl and ^{79}Br. ^{7}Li MAS NMR spectra were obtained using single pulse experiments with optimised pulse lengths of 4.8 μs.

5 Results and Discussions

Fluorinated LiRAPs are metastable and can decompose to form LiCl, LiOH, LiF and LiBr. Therefore, it was essential to see if fluorine-doping was possible. Data from the NMR was acquired using Bruker's TopSpin software. Sola and adjust phase tools were employed to phase the data. A python command was run to save the data text file, which was then plotted on Plot2 software.

The ^{7}Li NMR shows an increase in the line broadening, suggesting that the OH^- ions can be replaced by F^- ions. However, after ~ x = 0.6 fluorine, no doping is taking place as the line-broadening halts. Gaussian curves were used as fitted plots to find an accurate fit to the data. It was found that two Gaussian curves were enough to find a good overlap for the data using iteration.

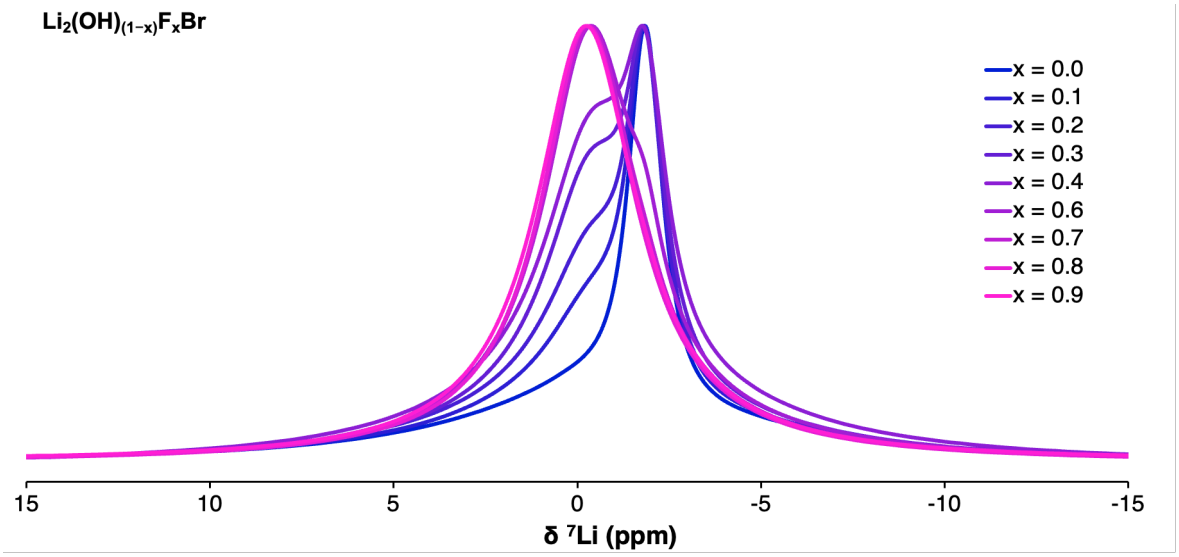

Figure 7: ^{7}Li MAS NMR spectra acquired for $Li_2(OH)_{(1-x)}F_xBr$.

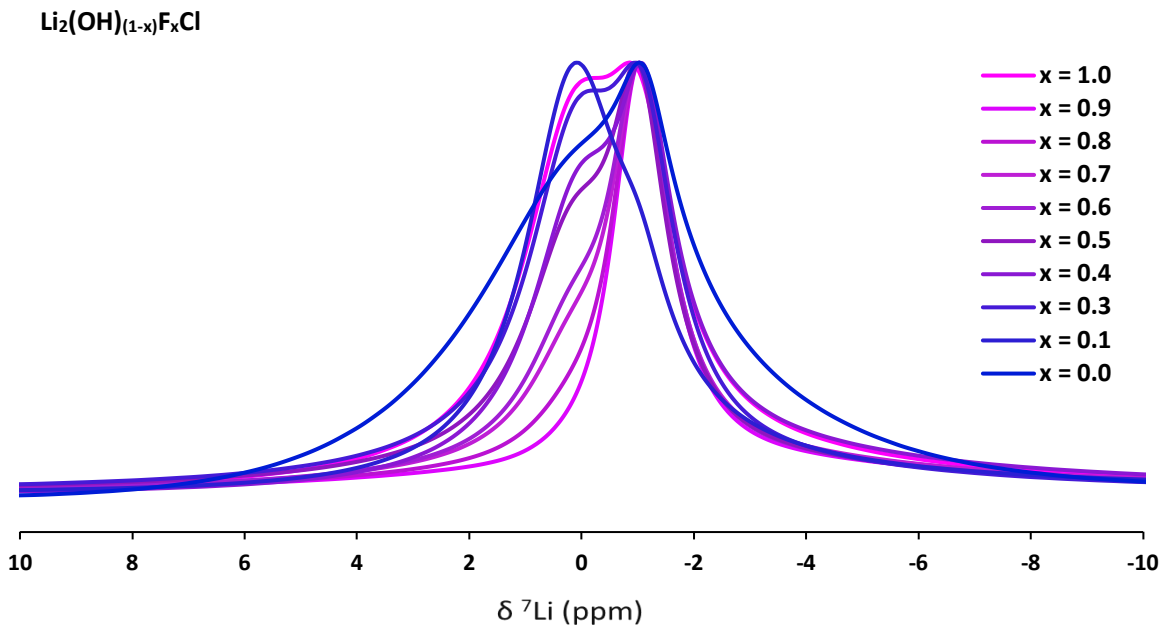

Figure 8: ^{7}Li MAS NMR spectra acquired for $Li_2(OH)_{(1-x)}F_xCl$.

Temperature-varied solid state NMR experiments could be employed in the future to observe how the ionic conductivity of the sample changes over time, therefore highlighting the change in material structure. Broad single resonance peak with two sets of spinning sidebands is characteristic of OH groups. At lower temperatures, the plot would be characteristic of room temperature phase of Li_2OHCl, *i.e.*, a relatively broad resonance with two sets of spinning sidebands would be observed. As the temperature is raised, the resonance plot would exhibit an increase in intensity, with a reduction in intensity for the spinning sidebands. Further increase in temperature (around 100 °C) would exhibit narrower lineshapes and even greater intensities. Furthermore, XRD patterns could be used to find the determine groups and phase groups of the sample, along with identifying reflections of the starting materials which haven't been incorporated into the final product. Reitveld analysis and refinement using the acquired XRD data and the *Pm*3*m* ($Li_2(OH)_{0.9}F_{0.1}Cl$), *Pban* (Li_2OHCl) and *Fm*3*m* (LiCl and LiF) structural models help identify the quality of the fit and the match between calculated and observed reflection intensities using χ^2 statistical test. Thus, the effect fluorine-doping on

stabilisation of the cubic phase could be confirmed. Proton and Bromine NMR experiments are currently being conducted and results of these will be underway.

6 Conclusion

To conclude, the data presented in this report demonstrates that fluorine-doping of lithium solid-state electrolytes is a promising candidate to improve ionic conductivity, and hence the energy density of Lithium-ion Solid-State Batteries. However, further research needs to be conducted for large scale production of Fluorine-doped batteries, good compatibility with the anode and cathode active materials, cost efficiency and cycle time. Energy level alignment considerations such as conduction band, valence band, Fermi level, and work function between the electrodes must also be kept in mind.[14] Although very energy dense, lithium is a finite source. Sodium batteries provide and alternative source due to their high performance, energy density and reduced thermal runaway due to a larger ionic radius; these are being researched widely recently. Albeit there are very few mechanistic similarities between lithium and sodium batteries, the link between their mechanisms is still being research.

7 References

[1] Yan S., Yim C.-H., Pankov V., Bauer M., Baranova E., Weck A., Merati A., Abu-Lebdeh Y., Perovskite Solid-State Electrolytes for Lithium Metal Batteries, *Batteries,* 2021, *7*, 75

[2] Da D., Li-ion batteries: basics, progress, and challenges, *Energy Science and Engineering,* 2015, **3**, 385–418

[3] Naoki N., Feixiang W., Jung T.L., Gleb Y., Li-ion battery materials: present and future, *Materials today,* 2015, **18**, 5, 252 – 264

[4] Jakob A., Tobias E., Matthias K., Arefeh K., Zhen C., Dominic B., *Sustainable Energy Fuels,* 2020**, 4**, 5387 – 5416

[5] Zeyu X., Xiuling S., Xiaoqiang Z., Zihan W., Sheng S., Kaikai L., Tong-Yi Z/g, Chemical Strain of Graphite-Based Anode during Lithiation and Delithiation at Various Temperatures, *Science Partner Journals,* 2021, doi: 10.34133/2021/9842391

[6] Ran W., Shaojie C., Tianyi G., Wei L., Challenges, fabrications and horizons of oxide solid electrolytes for solid-state lithium batteries, *NanoSelect,* **2021,** 2, 2256 – 2274

[7] Fan L., Wei S., Li S., Li Q., Lu. Y, Recent progress of the solid-state electrolytes fro high-energy metal-based batteries, *Advanced Energy Matter,* doi: 10.1002/aenm.201702657

[8] C. M. Julien, *Solid State Ionics*, 2006, **177**, 11–19

[9] Liguang W., Jun L., Guolong L., Wenyan L., Qiqi T., Caihong S., Huile J., Guang C., Shun W., Fundamentals of Electrolytes for Solid-State Batteries: Challenges and Perspectives, *frontiers in Materials*, 2020, doi: 10.3389/2020/00111

[10] James A. D., Theodosios E., Karen E. J., Anti-perovskites for solid-state batteries: recent developments, current challenges and future prospects, *Journal of Materials Chemistry,* 2021, **9**, 18746 – 18772

[11] Dr. Yutao Li, Dr. Weidong Xhou, Dr. Sen Xin, Dr. Shuai Li, Dr. Jinlong Zhu, Dr. Xujie Lü, Dr. Zhimming Cui, Prof. Quanxi Jia, Prof. Jianshi Zhou, Prof. Yusheng Zhao, John B. Goodenough, Fluorine-Doped Antiperovskite Electrolyte for All-Solid-State Lithium-Ion Batteries, *Angewandte Chemie,* 2016**, 55**, 9965 – 9968

[12] Lihong Yin, Huimin Yuan, Long Kong, Zhouguang Lu, Yusheng Zhao, Engineering Frenkel defects of anti-perovskite solid-state electrolytes and their applications in all-solid-state lithium-ion batteries, *ChemComm,* 2020, **56**, 1251

[13] Gerald Schubert, Geomagnetics Induction Studies, *Treatise on Geophysics,* 2015, **5**, 219 - 254

[14] Taehoon Kim, Wentao Song, Dae-Yong Song, Luis K. Ono, Yabing Qi, Lithium-ion batteries: an outlook on present, future, and hybridised technologies, *Energy Materials and Surface Sciences,* 2019, **7**, 2942 – 2964